Deletion of Cd39/Entpd1 Results in Hepatic Insulin Resistance

Keiichi Enjyoji,[1] Ko Kotani,[2] Chandrashekar Thukral,[1] Benjamin Blumel,[1] Xiaofeng Sun,[1] Yan Wu,[1] Masato Imai,[1] David Friedman,[1] Eva Csizmadia,[1] Wissam Bleibel,[1] Barbara B. Kahn,[2] and Simon C. Robson[1]

OBJECTIVE—Extracellular nucleotides are important mediators of inflammatory responses and could also impact metabolic homeostasis. Type 2 purinergic (P2) receptors bind extracellular nucleotides and are expressed by major peripheral tissues responsible for glucose homeostasis. CD39/ENTPD1 is the dominant vascular and immune cell ectoenzyme that hydrolyzes extracellular nucleotides to regulate purinergic signaling.

RESEARCH DESIGN AND METHODS—We have studied Cd39/Entpd1-null mice to determine whether any associated changes in extracellular nucleotide concentrations influence glucose homeostasis.

RESULTS—Cd39/Entpd1-null mice have impaired glucose tolerance and decreased insulin sensitivity with significantly higher plasma insulin levels. Hyperinsulinemic-euglycemic clamp studies indicate altered hepatic glucose metabolism. These effects are mimicked in vivo by injection into wild-type mice of either exogenous ATP or an ecto-ATPase inhibitor, ARL-67156, and by exposure of hepatocytes to extracellular nucleotides in vitro. Increased serum interleukin-1β, interleukin-6, interferon-γ, and tumor necrosis factor-α levels are observed in Cd39/Entpd1-null mice in keeping with a proinflammatory phenotype. Impaired insulin sensitivity is accompanied by increased activation of hepatic c-Jun NH_2-terminal kinase/stress-activated protein kinase in Cd39/Entpd1 mice after injection of ATP in vivo. This results in decreased tyrosine phosphorylation of insulin receptor substrate-2 with impeded insulin signaling.

CONCLUSIONS—CD39/Entpd1 is a modulator of extracellular nucleotide signaling and also influences metabolism. Deletion of Cd39/Entpd1 both directly and indirectly impacts insulin regulation and hepatic glucose metabolism. Extracellular nucleotides serve as "metabolokines," indicating further links between inflammation and associated metabolic derangements. ***Diabetes*** **57:2311–2320, 2008**

Purinergic signaling elements comprise a ubiquitous sensing network within the extracellular environment. In this system, extracellular nucleotides, such as ATP, ADP, and UTP, and extracellular nucleosides, such as adenosine, trigger differential cellular responses (1,2). Purinergic signaling pathways require extracellular nucleotide release mechanisms, purinergic receptors for these mediators (type 2 purinergic [P2] receptors), and regulated expression of ectonucleotidases that hydrolyze extracellular nucleotides to generate adenosine (3–5). Extracellular nucleotides are provided by the secretion/release of intracellular substrates, and levels are increased in hypoxia, injury, mechanical stress, and inflammation.

Several reports suggest roles for extracellular nucleotides and nucleosides in glucose homeostasis (e.g., stimulation of insulin secretion from islets [6–8], modulation of glucose uptake [9,10]). P2 receptors are expressed by insulin-sensitive tissues and also by immune cells. Extracellular nucleotides activate inflammatory pathways, inducing expression of proinflammatory cytokines including interleukin-1 (11), interferon-γ (12), and activating inflammatory kinase such as c-Jun NH_2-terminal kinase (c-JNK) through the activation of P2 receptors (13,14). Protein kinase C can be also activated by these pathways (15). These kinases phosphorylate serine residues of insulin receptor substrate (IRS)-1/2, resulting in impaired insulin signaling by precluding tyrosine phosphorylation required to recruit phosphoinositide 3-kinase (16,17).

CD39/ENTPD1 is an ectoenzyme that hydrolyzes extracellular nucleotides and is predominantly expressed in vascular endothelial cells and immune cells. We have previously shown that deletion of Cd39/Entpd1 results in disordered purinergic signaling responses that compromise vascular thromboregulation and augment inflammatory responses (3,5,12). Here, we show that Cd39/Entpd1-null mice demonstrate impaired glucose tolerance secondary, at least in part, to hepatic insulin resistance. This phenomenon is associated with increased levels of hepatocyte c-JNK activation in response to extracellular nucleotides, resulting in aberrant IRS-2 phosphorylation within the livers of the mutant mice. Our studies clearly establish links between extracellular nucleotide–mediated regulation of glucose metabolism and inflammation that are uniquely influenced by the vascular expression of Cd39/Entpd1.

From the [1]Liver Center, Department of Medicine, Beth Israel Deaconess Medical Center, Harvard Medical School, Boston, Massachusetts; and the [2]Division of Endocrinology, Diabetes and Metabolism, Department of Medicine, Beth Israel Deaconess Medical Center, Harvard Medical School, Boston, Massachusetts.

Corresponding author: Keiichi Enjyoji, kenjoji@bidmc.harvard.edu.

Received 6 September 2007 and accepted 11 June 2008.

Published ahead of print at http://diabetes.diabetesjournals.org on 20 June 2008. DOI: 10.2337/db07-1265.

RESEARCH DESIGN AND METHODS

Cd39/Entpd1-null mice have been described in detail elsewhere (3) and were backcrossed six times onto the C57BL/6 genetic background. C57BL/6 wild-type mice were obtained from Taconic. Male mice were used in all experiments. Mice were housed under conditions of controlled temperature and illumination (12-h light cycle, lights on at 0700 h). Unless otherwise stated, mice were fed a normal diet ad libitum. All research and animal care protocols were approved by the Beth Israel Deaconess Medical Center Animal Experimentation Ethics Committee.

Glucose tolerance and insulin tolerance tests. A glucose tolerance test (GTT) was carried out with overnight-fasted (16 h) mice at 9 and 16 weeks old. GTT was performed by intraperitoneal injection of glucose (1 g D-glucose/kg body wt). An insulin tolerance test (ITT) was performed by intraperitoneal injection of human regular insulin (0.75 units insulin/kg body wt; Eli Lilly) at

2 h after removal of food. Blood glucose levels were determined with the OneTouch Ultra blood glucose–monitoring system (LifeScan). To determine effects of exogenous nucleotides on GTT, 7-week-old wild-type mice were fasted overnight. After basal plasma glucose was measured, the experimental mice were injected with ATP, ADP, UTP, or UDP solution (0.5 mmol/kg body wt) intraperitoneally, whereas control animals were administered saline. At 30 min, each animal was subjected to a GTT (n = 5–6 per group). The effects of an ecto-ATPase inhibitor, ARL-67156 (5 mg/kg body wt), on the GTT were examined in a similar manner.

Hyperinsulinemic-euglycemic clamp study. Hyperinsulinemic-euglycemic clamp studies were performed on 16- to 17-week-old mice. Four days before experiments, an indwelling catheter was inserted in the right internal jugular vein of experimental animals. After an overnight fast, a 120-min hyperinsulinemic-euglycemic clamp was conducted in awake mice, as previously described (18). Infusions of human insulin (Eli Lilly) at a rate of 15 pmol · kg^{-1} · min^{-1} raised plasma insulin levels to ~900 pmol/l (wild type: 863.0 ± 151.4 pmol/l [n = 8], knockout: 890.3 ± 108.4 pmol/l [n = 8]; P = 0.8741), and 40% glucose was infused at variable rates to clamp the plasma glucose levels at ~6.5 mmol/l using microdialysis pumps. At the end of the clamp studies, each tissue was harvested and frozen in liquid nitrogen. Clamp results were analyzed as described previously (18).

Measurements of metabolites, serum hormones, and cytokines. Insulin concentrations were determined using a rat insulin enzyme-linked immunosorbent assay (ELISA) kit with mouse insulin standards (Crystal Chem). Serum triglyceride and free fatty acid concentrations were measured using a colorimetric kit (Sigma-Aldrich) and a NEFA-C kit (Wako Chem), respectively. Serum 3-hydroxybutyric acid levels were determined using a colorimetric assay kit (Wako Chem). Plasma leptin was measured using a mouse leptin ELISA kit (Crystal Chem) and a mouse adiponectin radioimmunoassay kit (Linco Research). Urine catecholamine levels were determined by an ELISA kit (Alpco Diagnostics). Serum cytokine levels (interleukin-1β, interleukin-6, interferon-γ, and tumor necrosis factor-α) were measured by ELISA (eBiosciences).

Measurements of nuclear factor-κB p65. Liver nuclear extracts were prepared with the Nuclear Extract Kit (Active Motif), according to the manufacturer's instruction. Nuclear factor-κB (NFκB) p65 levels in equal amounts of nuclear extracts were determined with TransAM NFκBp65 (Active Motif).

Body composition. A PIXIMUS Densitometer (LUNAR) was used for the measurement of body composition in anesthetized mice (19).

Indirect calorimetry and daily activity. In vivo indirect calorimetry was performed in metabolic chambers using an Oxymax system (Columbus Instruments) in mice at 16–17 weeks old. To calculate oxygen consumption (V_{O_2}), carbon dioxide production (V_{CO_2}), and RQ (ratio of V_{CO_2} to V_{O_2}), gas concentrations were monitored at the inlet and outlet of the sealed chambers. Global daily activity was monitored by counting the number of times that an individual mouse blocked an infrared beam running along x- and y-axes inside an individual cage.

Isolation and culture of hepatocytes. Hepatocytes were isolated from 7-week-old mice according to the method of Harman et al. (20). Hepatocytes were further purified by centrifugation with Percoll and plated onto gelatin-coated dishes. Unattached cells were removed at 6 h. The cells were used for experiments at 24-h postisolation.

Glucose uptake by cultured hepatocytes. Primary murine hepatocytes were plated onto six-well plates at 4 × 10^5 cells/well. The cells were cultured in a 37°C CO_2 incubator in William's E buffer with 10% FCS. Subsequently, cells were serum starved overnight in William's E buffer with 0.1% BSA. The cells were washed twice with Krebs-Ringer/Pi/Hepes (KRPH) and treated with either 100 nmol/l insulin or KRPH buffer (control) for 30 min at 37°C, followed by addition of 10 mmol/l 2-deoxy-D-glucose (2-DG) containing 0.3 mCi/ml 2-deoxy-D-[^{3}H]glucose. After a 10-min incubation, the cells were washed with ice-cold PBS three times, air dried, then lysed with ice-cold 0.2 N NaOH. Radioactivity was determined by scintillation counting, and protein concentrations were determined using the Bio-Rad DC protein assay. 2-DG uptake was expressed as cpm · mg^{-1} · ml^{-1} of protein concentration. Similar protocol was used to measure 2-deoxy-D-[^{3}H]glucose uptake in wild-type cells that were

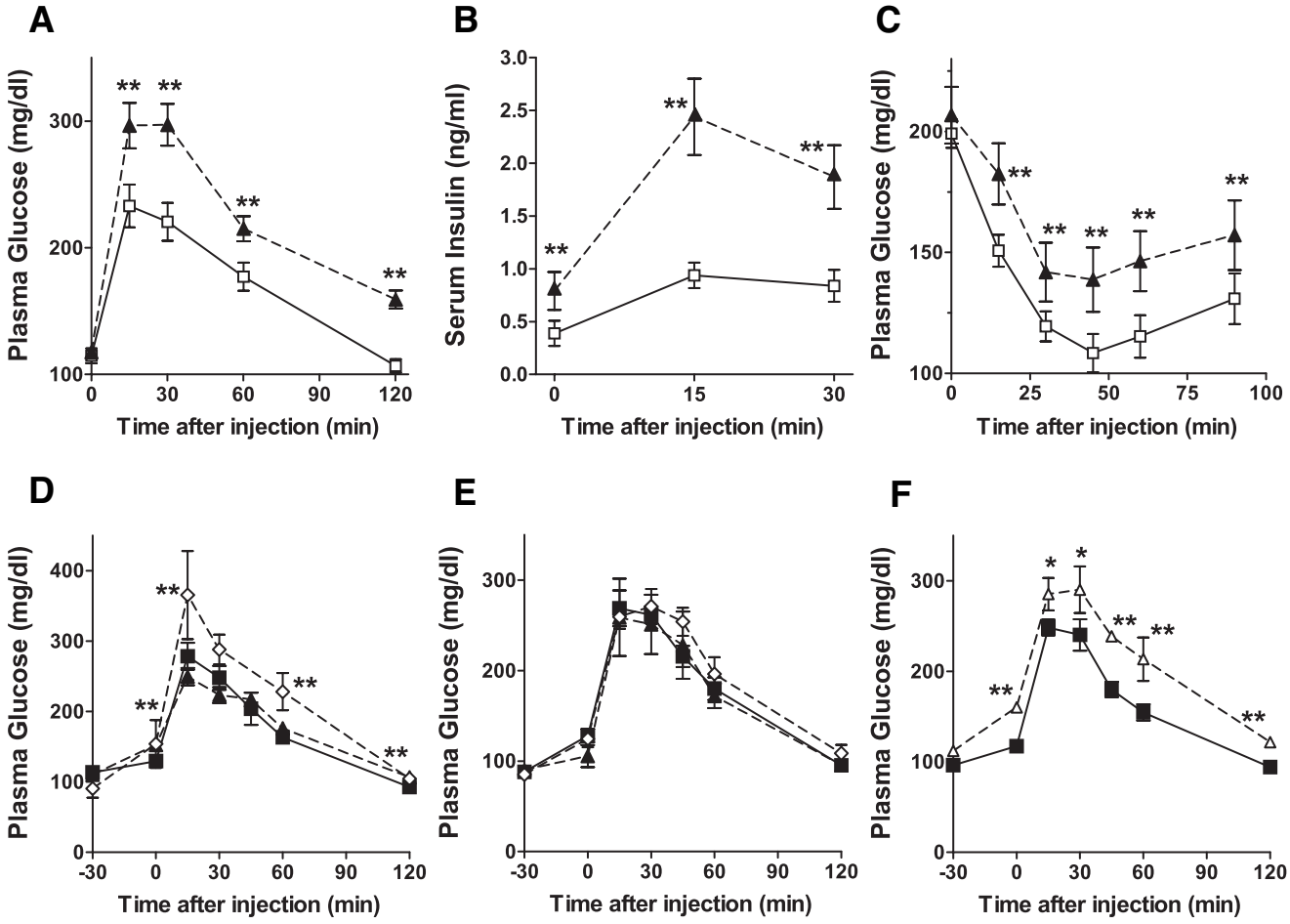

FIG. 1. Cd39/Entpd1$^{-/-}$ mice exhibit impaired glucose tolerance and insulin resistance. *A*: GTT. *B*: Plasma insulin levels during GTT. *C*: ITT. ▲, Cd39/Entpd1$^{-/-}$ mice; □, wild-type mice (9 weeks old, n = 6). *D–F*: Effects of different nucleotides on GTT in wild-type mice (n = 5–6). *D*: ◇, ATP-treated mice; ▲, UTP-treated mice; ■, saline control. *E*: ◇, ADP-treated mice; ▲, UDP-treated mice; ■, saline control. *F*: △, ARL-67156–treated mice; ■, saline control. Data are means ± SE. **P < 0.05; *P < 0.1.

TABLE 1
Comparison of blood analysis data of Cd39/Entpd1$^{-/-}$

	Wild type	Cd39/Entpd1$^{-/-}$	*P*
Body weight (g)			
9 weeks (fasting)	24.6 ± 0.3	25.3 ± 0.9	0.426
9 weeks (fed)	26.6 ± 0.4	27.3 ± 0.9	0.418
16 weeks (fasting)	27.2 ± 0.3	29.1 ± 1.1	0.11
16 weeks (fed)	30.2 ± 0.4	31.6 ± 1.0	0.24
Fasting glucose (mg/dl)			
9 weeks	95 ± 5	97 ± 6	0.426
16 weeks	105 ± 3	104 ± 2	0.331
Fed glucose (mg/dl)			
9 weeks	185 ± 8	190 ± 6	0.418
16 weeks	189 ± 3.7	202 ± 8.1	0.09
Fasting insulin (pg/ml)			
9 weeks	0.34 ± 0.07	0.38 ± 0.13	0.791
16 weeks	0.39 ± 0.12	0.79 ± 0.18	0.028
Fed insulin (pg/ml)			
9 weeks	1.51 ± 0.07	2.02 ± 0.22	0.0366
16 weeks	0.74 ± 0.05	1.74 ± 0.24	0.005
Fasting triglycerides (mg/dl)			
9 weeks	35 ± 9	47 ± 4	0.252
15 weeks	60 ± 4	65 ± 5	0.225
35 weeks	45 ± 4	95 ± 15	0.01
Fed triglycerides (mg/dl)			
9 weeks	57 ± 6	57 ± 4	0.976
16 weeks	40 ± 5	54 ± 5	0.067
Fasting free fatty acids (mmol/l)			
9 weeks	1.08 ± 0.07	0.98 ± 0.04	0.261
15 weeks	1.21 ± 0.05	1.17 ± 0.03	0.492
35 weeks	0.71 ± 0.04	1.01 ± 0.11	0.013
Fed free fatty acids (mmol/l)			
9 weeks	0.49 ± 0.02	0.53 ± 0.02	0.135
16 weeks	2.94 ± 0.08	3.14 ± 0.13	0.212
Fasting 3-hydroxybutyrate (mmol/l)			
15 weeks	1.58 ± 0.05	1.64 ± 0.05	0.453
Leptin (ng/ml)			
16 weeks	12.1 ± 0.8	18.6 ± 2.8	0.036
Adiponectin (μg/ml)			
16 weeks	9.1 ± 0.6	8.7 ± 0.4	0.623
Visceral fat (% of body wt)			
16 weeks	25.3 ± 0.7	27.2 ± 1.9	0.352
Total fat (%)			
16 weeks	24.6 ± 0.5	27.0 ± 1.9	0.131
Serum cytokines (15 weeks, fasting)			
Interleukin-1β (pg/ml)	1.16 ± 0.88	8.05 ± 3.43	0.049
Interferon-γ (pg/ml)	41.5 ± 6.2	80.6 ± 10.5	0.01
Interleukin-6 (Pg/ml)	1.71 ± 0.75	5.14 ± 1.61	0.037
Tumor necrosis factor-α (arbitrary units)	N.D (below range)	1.53 ± 0.45	<0.05

Data are mean ± SE from 6–10 animals of each group.

either pretreated with 100 μmol/l ATP or KRPH buffer for 30 min before commencing the insulin-stimulated 2-DG uptake assay.

Measurement of gluconeogenesis in cultured hepatocytes. Primary hepatocytes were serum starved overnight in DMEM with 0.4% FCS and 5 mmol/l D-glucose, washed three times with KRPH buffer, and incubated with KRPH buffer containing 20 mmol/l lactate and 2 mmol/l pyruvate (basal) or KRPH buffer containing either 10 nmol/l insulin or 100 nmol/l insulin with 20 mmol/l lactate and 2 mmol/l pyruvate. Glucose content in each aliquot was measured using an Amplex Red Glucose Assay (Invitrogen). Glucose production was expressed as measured fluorescence · mg^{-1} · ml^{-1} of protein concentration. Similar experimental protocol was used to measure glucose production in wild-type cells that were either pretreated with 100 μmol/l ATP or KRPH buffer for 30 min before commencing the insulin-stimulated gluconeogenesis assay.

Western blotting. Tissue or cell lysates were prepared in the lysis buffer as described previously (18). Clarified supernatant was separated on SDS-PAGE under reducing condition and then transferred to polyvinylidene fluoride membrane for Western blot analysis. For IRS-1 and -2 studies, 500 μg of cleared lysate was incubated with anti–IRS-1 or anti–IRS-2 antibodies (Upstate) then captured with protein-A/G Sepharose beads (Sigma-Aldrich). After washing the beads, IRS-1 or -2 was eluted in SDS-loading buffer and subjected to Western blot analysis with anti–phosphotyrosine antibody or anti–IRS-1 or anti–IRS-2 antibodies. Images were taken on a Kodak chemiluminescent image station 2000MM and quantified with an accompanying software program (Kodak). Detection of either phospho-JNK or JNK was carried out using anti–*p*-JNK antibody or anti-JNK antibody (Cell Signaling Technolgies). Phospho-Ser731–IRS-2 was detected using specific antibodies purchased from Abcam.

Administration of ATP into portal vein. Twelve-week-old male mice were anesthetized with nembutal then 10 mmol/l ATP, and PBS was administered via a portal vein at 1.4 μl/g and at 2.5 s/g body wt using a microinfusion pump. At 30 min of infusion, mice were killed by exsanguination, and immediately the perfused liver was snap frozen in liquid nitrogen.

Immunohistochemistry. Animals were anesthetized with avertin and killed by exsanguination. Pancreatic, hepatic, and skeletal muscle tissues were immediately embedded in OCT compound in an isopentene–liquid nitrogen

freezing bath. Brown adipose tissue (BAT) was fixed in zinc fixative solution (BD Biosciences) for 1.5 days. The tissue sections were used for immunohistochemical staining with antibodies against Cd39/Entpd1 (3), Cd31 (BD Biosciences), insulin, and glucagon (Dako).

Real-time PCR for gluconeogenetic enzymes. Liver total RNA was purified with a Qiagen RNAeasy mini-kit and used to synthesis cDNA using an Invitrogen first-strand cDNA synthesis kit. Real-time PCR was performed with a iTaq SYBR Green Supermix with ROX (Bio-Rad) on a Stratagene MX3000P quantitative PCR system. The primers used were TGGTAGCCCTGTCTTTC TTTG and TTCCAGCATTCACACTTTCCT for glucose-6-phosphatase and ACACACACACATGCTCACAC and ATCACCGCATAGTCTCTGAA for phosphoenolpyruvate carboxylase (21). Actin values were used for normalization.

RESULTS

Cd39/Entpd1 deletion results in abnormalities in GTTs and ITTs. Cd39/Entpd1 knockout (Cd39/Entpd1$^{-/-}$) mice were subjected to GTTs and ITTs at 9 weeks of age (Fig. 1). Blood glucose levels were significantly higher in Cd39/Entpd1$^{-/-}$ mice throughout the GTT when compared with wild-type mice (Fig. 1*A*). Plasma insulin levels during the GTT were also consistently higher in Cd39/Entpd1$^{-/-}$ mice when compared with wild-type mice, suggesting insulin resistance in Cd39/Entpd1$^{-/-}$ mice (Fig. 1*B*). Cd39/Entpd1$^{-/-}$ mice also exhibited impaired responses to insulin during the ITT (Fig. 1*C*). Cd39/Entpd1$^{-/-}$ mice at 16 weeks likewise exhibited glucose intolerance and insulin resistance as determined by a GTT and ITT. There were no differences in fasting- and fed-state blood glucose levels between Cd39/Entpd1$^{-/-}$ and wild-type mice.

We then examined effects of exogenous nucleotide administration upon a GTT in wild-type mice. Increases in blood glucose levels were observed at 30 min after administration of ATP versus saline (Fig. 1*D*). These plasma glucose increments were sustained in the group treated with ATP during the GTT. The preadministration of other nucleotides, UTP, ADP, and UDP, did not substantially affect glucose tolerance in wild-type mice (Fig. 1*D* and E). Preadministration of ARL-67156, a competitive ecto-ATPase inhibitor, resulted in increases in glucose levels basally and following a GTT in wild-type mice (Fig. 1*F*).

Metabolic parameters. Insulin resistance is often accompanied by obesity and disordered lipid metabolism. We therefore assessed other parameters relevant to these disorders of metabolism (Table 1). Cd39/Entpd1$^{-/-}$ mice are clearly not obese. Plasma insulin levels were significantly higher in fed Cd39/Entpd1$^{-/-}$ mice at all ages tested and in fasting Cd39/Entpd1$^{-/-}$ mice at 16 weeks of age. Plasma free fatty acid and triglyceride levels in Cd39/Entpd1$^{-/-}$ mice were not generally different from wild-type mice but became statistically higher at 35 weeks of age. Plasma leptin levels of Cd39/Entpd1$^{-/-}$ mice were significantly higher than in wild-type mice, but adiponectin levels were comparable. Plasma 3-hydroxybutyrate levels were comparable in Cd39/Entpd1$^{-/-}$ mice and wild-type mice.

We also examined sympathetic reactivity in Cd39/Entpd1e$^{-/-}$ mice. Total adrenaline and noradrenaline levels in urine were not statistically different between these two groups (adrenaline: Cd39/Entpd1$^{-/-}$ mice 1.49 ± 0.50 pg/day vs. wild-type mice 1.64 ± 0.48 pg/day, $P = 0.83$; noradrenoline: Cd39/Entpd1$^{-/-}$ mice 2.76 ± 0.90 pg/day vs. wild-type mice 3.06 ± 0.73 pg/day, $P = 0.79$).

Energy expenditure and activity. We examined the impact of Cd39/Entpd1 deletion on energy metabolism (Fig. 2). Heat generation (Fig. 2*A*), oxygen consumption (Fig. 2*B*), and respiratory ratio ((Fig. 2*C*) were significantly lower in Cd39/Entpd1$^{-/-}$ mice, both during dark and light periods. However, food intake and daily activities of Cd39/Entpd1$^{-/-}$ mice were comparable with those of wild-type mice (Fig. 2*D*).

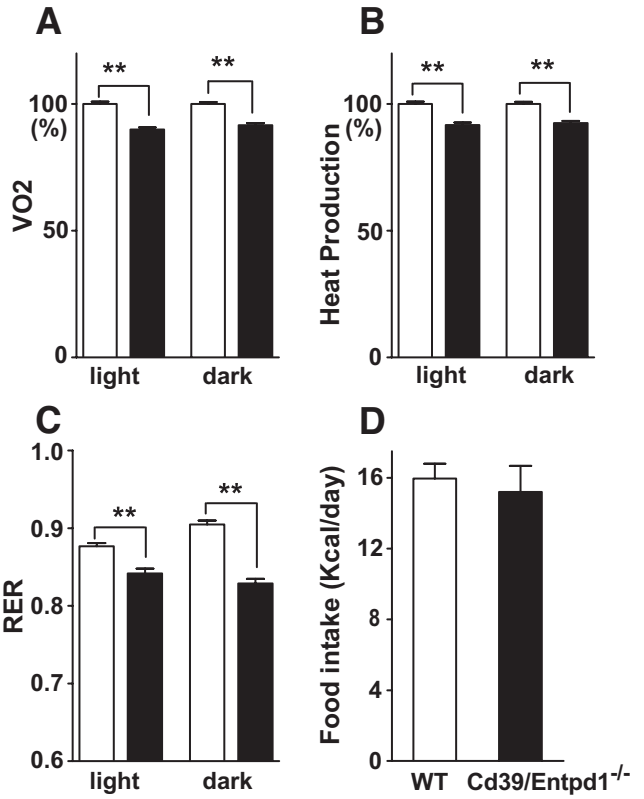

FIG. 2. Calorimetric and functional analyses of Cd39/Entpd1$^{-/-}$ mice. Cd39/Entpd1$^{-/-}$ mice showed decreased energy expenditure. Food uptake did not differ between Cd39/Entpd1$^{-/-}$ and wild-type mice. *A*: Oxygen consumption. *B*: Heat generation. *C*: Respiratory ratio. *D*: Accumulated food intake over 3 days ($n = 6$ for wild-type -WT] mice and $n = 7$ for Cd39/Entpd1$^{-/-}$ mice). Results were analyzed using data from 3 consecutive days. Data are means ± SE. **$P < 0.05$.

Hyperinsulinemic-euglycemic clamp studies. To analyze systemic glucose uptake and usage, we performed hyperinsulinemic-euglycemic clamp studies. Glucose uptake in the extrahepatic tissues was not statistically different between Cd39/Entpd1$^{-/-}$ and wild-type mice (Fig. 3*A*). Glucose infusion rates during the glucose clamp were, however, significantly lower in Cd39/Entpd1$^{-/-}$ mice (Fig. 3*B*). Coincidently, glucose disappearance rates (R_d) were lower in Cd39/Entpd1$^{-/-}$ mice (Fig. 3*C*). Basal hepatic glucose production was normal, but the extent of insulin-dependent suppression of hepatic glucose production was significantly decreased in Cd39/Entpd1$^{-/-}$ mice (Cd39/Entpd1$^{-/-}$ mice: 26.6 ± 14.4% vs. wild-type mice: 69.5 ± 9.6%; $P = 0.021$) (Fig. 3*D*). These results suggest that systemic insulin resistance and glucose intolerance of Cd39/Entpd1$^{-/-}$ mice were associated with impaired hepatic responses to insulin and decreased R_d.

Phosphoenolpyruvate carboxylase and glucose-6-phosphatase expression by RT-PCR were significantly higher in fasting Cd39/Entpd1$^{-/-}$ mice liver than in wild-type mice liver (phosphoenolpyruvate carboxylase: Cd39/Entpd1$^{-/-}$ mice 128.8 ± 10.2% vs. wild-type mice 100.0 ± 0.6%, $P = 0.027$; glucose-6-phosphatase: Cd39/Entpd1$^{-/-}$ mice 240.6 ± 26.1% vs. wild-type mice 100.0 ± 7.3%, $P = 0.001$).

Localization of Cd39/Entpd1 in mouse liver, pancreas, BAT, and skeletal muscle. High levels of Cd39/Entpd1 staining were observed in the endothelium with

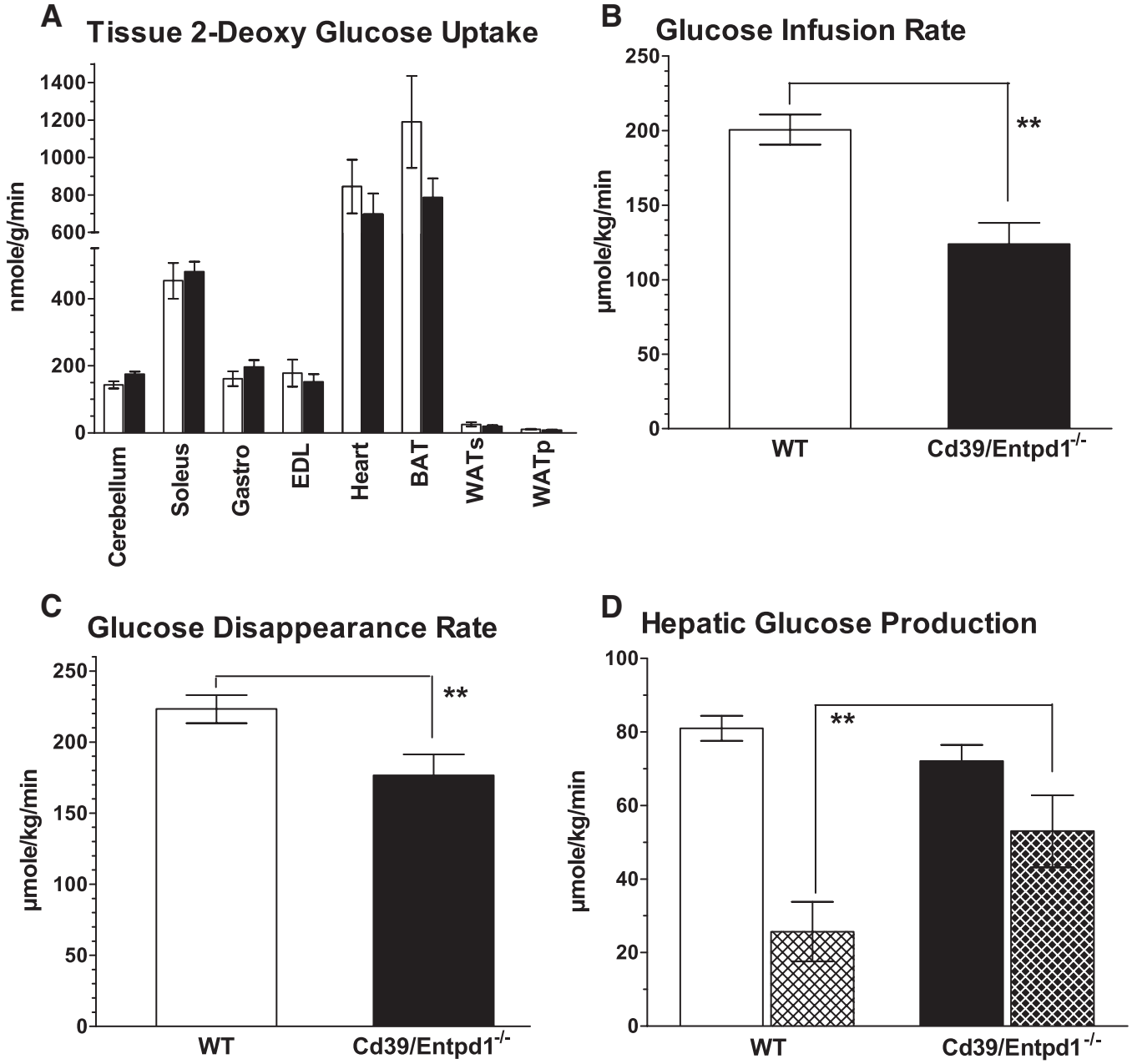

FIG. 3. Cd39/Entpd1$^{-/-}$ mice manifest impaired hepatic glucose homeostasis during hyperinsulinemic-euglycemic clamp. *A*: Tissue glucose uptake estimated by 2-DG. *B*: Glucose infusion rate. *C*: Glucose disappearance rate (R_d). *A–C*: ■, Cd39/Entpd1$^{-/-}$ mice; □, wild-type (WT) mice. *D*: Hepatic glucose production and its suppression by insulin. ■, Cd39/Entpd1$^{-/-}$ mice ; □, wild-type (WT) mice; ▨, with insulin (n = 6 for wild-type and n = 7 for Cd39/Entpd1$^{-/-}$ mice); solid bars, basal. Data are means ± SE. **P < 0.05.

the same expression in vascular smooth muscle cells of muscularized blood vessels within liver and skeletal muscle. Hepatic sinusoidal endothelial cells do not express Cd39/Entpd1 under basal conditions; however, Cd39/Entpd1 is expressed by certain hepatic sinusoidal cells (e.g., Kupffer cells and natural killer T-cells) (22,23).

Hepatocytes and skeletal muscle cells were negative for Cd39/Entpd1 (Fig. 4*A* and *B*). In brown adipose tissue, Cd39/Entpd1 expression was likewise restricted to the vascular endothelium of veins and arterioles but not noted in the microvasculature (Fig. 4*C*). In pancreas, the expression was also detected only in the vascular endothelial cells and vascular smooth muscle cells (Fig. 4*D* and *I*). In islets of Langerhans of the pancreas, the β-, α-, and δ-cells were all negative for Cd39/Entpd1. However, the microvasculature endothelial cells did stain for Cd39/Entpd1 in the pancreatic tissues and islets. Both wild-type and Cd39/Entpd1$^{-/-}$ islets stained for glucagon in a comparable manner (Fig. 4*K* and *O*); Cd39/Entpd1$^{-/-}$ islets reacted strongly for insulin (Fig. 4*L* and *P*).

Effect of extracellular ATP on glucose metabolism in hepatocytes. We next analyzed glucose metabolism in cultured primary hepatocytes isolated from Cd39/Entpd1$^{-/-}$ mice, as hyperinsulinemic-euglycemic clamp studies had suggested impaired hepatic glucose homeostasis in Cd39/Entpd1$^{-/-}$ mice. Overall glucose uptakes were significantly decreased in Cd39/Entpd1$^{-/-}$ hepatocytes in vitro (Fig. 5*A*).

The glucose uptake by wild-type hepatocytes was significantly decreased in the presence of ATP (Fig. 5*B*). Major contributions of liver to systemic glucose ho-

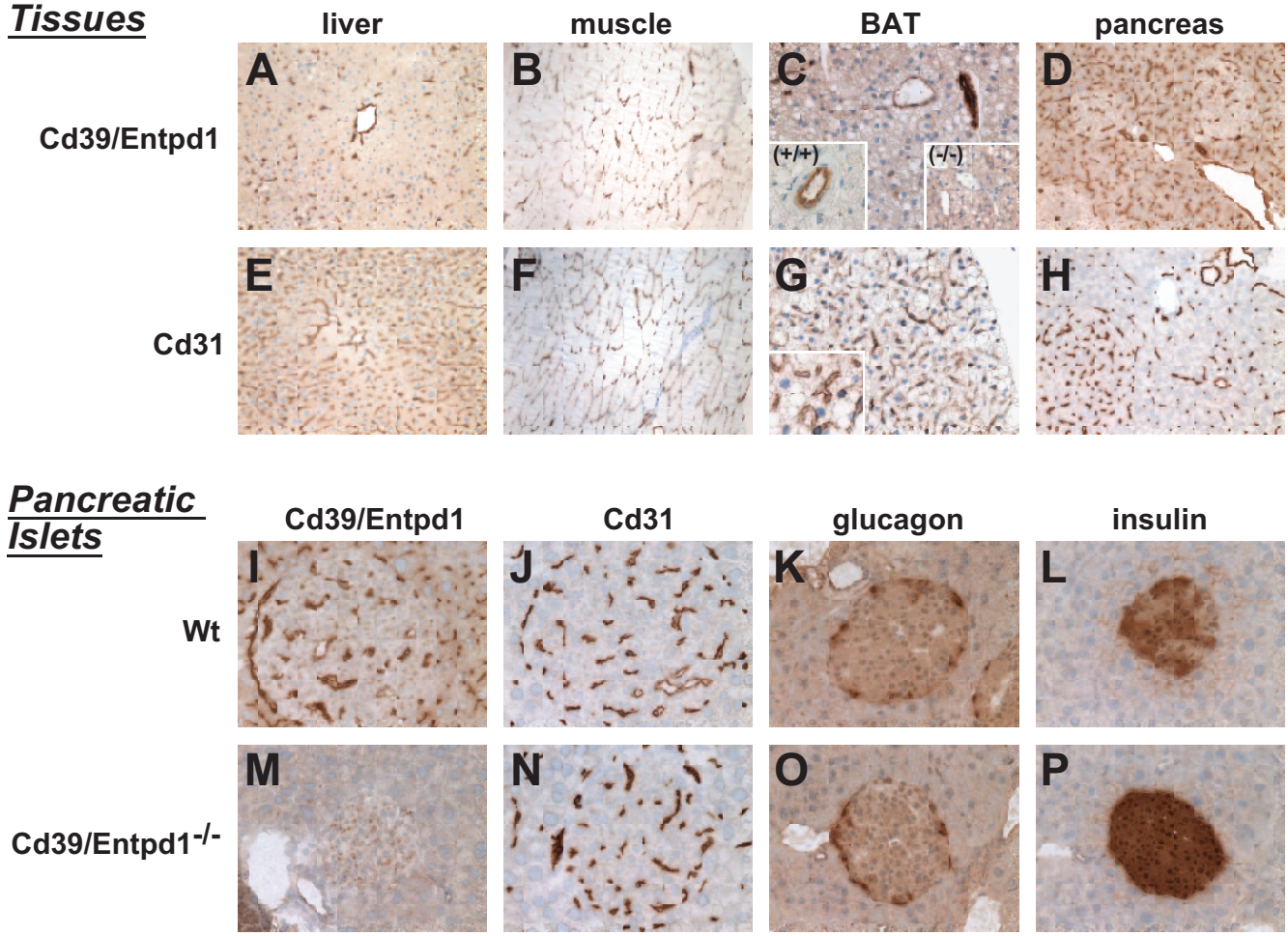

FIG. 4. Immunohistochemical analysis. Various insulin-sensitive tissues together with pancreatic islets were analyzed for Cd39 expression and are compared with the vascular endothelial marker Cd31. In the *lower right panels*, islet content of glucagon and insulin are also displayed. *A–D*, *I*, and *M*: Expression of Cd39/Entpd1. *E–H*, *J*, and *N*: Stained for Cd31. *A* and *E*: From wild-type liver. *B* and *F*: Wild-type skeletal muscle. *C* and *G*: Wild-type brown adipose tissue (BAT). *C*: *Inserted microimage*, at large magnification. ($^{+/+}$), wild-type BAT. ($^{-/-}$), Cd39/Entpd1-null BAT serves as a negative control. *D* and *H*: Wild-type pancreas. *I* and *J* are islet tissues from wild-type mice, whereas *M* and *N* are from the Cd39/Entpd1-null mice. *K* (wild type) and *O* (null) are stained for glucagon. *L* (wild type) and *P* (null) show the staining patterns for insulin (see text for details). (Please see http://dx.doi.org/10.2337/db07-1265 for a high-quality digital representation of this figure.)

meostasis involve regulation of glucose production that is suppressed by insulin. Glucose production was much higher in Cd39/Entpd1$^{-/-}$ hepatocytes than the wild-type hepatocytes. The increased level of glucose production by Cd39/Entpd1$^{-/-}$ hepatocytes was not significantly suppressed by insulin. In contrast, wild-type hepatocytes had the expected statistically significant suppression by insulin with respect to the glucose production (Fig. 5*C*). Exogenous extracellular ATP also induced higher levels of glucose production in wild-type hepatocytes; this was not suppressed by insulin (Fig. 5*D*).

Susceptibility of c-JNK phosphorylation by exogenous ATP treatment. c-JNK is a member of mitogen-activated protein kinase family that is activated by various proinflammatory cytokines. The activated c-JNK phosphorylates serine residues of IRS-1/2 and consequently prevents tyrosine phosphorylation of IRS-1/2 by insulin receptor (16). As extracellular ATP treatment induces c-JNK activation in rat hepatocytes (14), we examined phosphorylation levels of c-JNK in mouse liver after portal venous administration of ATP in vivo. We noted that phosphorylation of c-JNK in Cd39/Entpd1$^{-/-}$ mice liver at 30 min after ATP administration was significantly higher than in wild-type mice (Fig. 6*A*).

Decreased tyrosine phosphorylation of hepatic IRS-2 in Cd39/Entpd1$^{-/-}$ mice. Tyrosine phosphorylation of IRS could be hampered by phosphorylation of adjacent serine residues of IRS mediated by inflammatory kinase such as c-JNK or protein kinase C (16,17). Such kinases are activated through the activation of purinergic receptors by extracellular ATP (14,15). We therefore examined phosphorylation of IRS-1 and -2 in wild-type and Cd39/Entpd1$^{-/-}$ mice liver to dissect out differential responses to insulin in vivo. There were no differences in levels of tyrosine phosphorylation of IRS-1 between wild-type and Cd39/Entpd1$^{-/-}$ mice liver samples after insulin administration (Fig. 7). However, tyrosine phosphorylation of IRS-2 was markedly suppressed in Cd39/Entpd1$^{-/-}$ murine liver relative to wild-type samples postinjection of insulin. Relative levels of hepatic Ser-731 phosphorylation of IRS-2 were higher in Cd39/Entpd1$^{-/-}$ mice when compared with wild-type mice tissues (Fig. 7*D*).

Serum proinflammatory cytokine levels. Increased levels of proinflammatory cytokines are known to induce insulin resistance by activating kinases such as c-JNK. Extracellular nucleotides also clearly activate inflammatory pathways. Therefore, we have measured the serum levels of proinflammatory cytokines as surrogates for basal inflammatory responses in Cd39/Entpd1$^{-/-}$ mice.

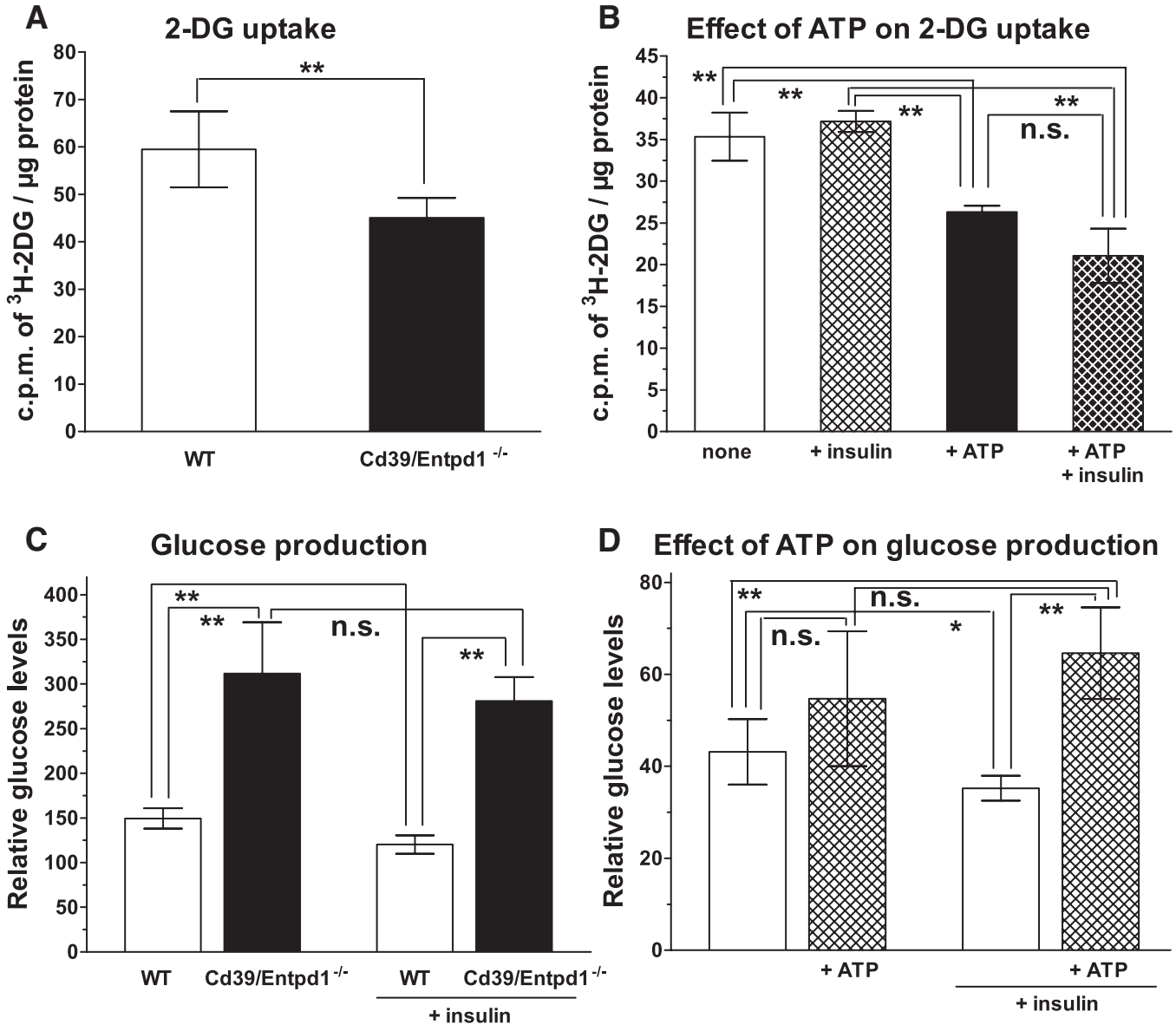

FIG. 5. Effect of extracellular ATP on glucose metabolism in hepatocytes. *A*: 2-DG uptake by Cd39/Entpd1$^{-/-}$ mice and wild-type (WT) mice hepatocytes. *B*: Effect of extracellular ATP on 2-DG uptake by wild-type mice hepatocytes. *C*: Hepatic glucose production of Cd39/Entpd1$^{-/-}$ mice and wild-type (WT) mice hepatocytes and its suppression by insulin. *D*: Effect of extracellular ATP on glucose production in wild-type hepatocytes. Experiment was performed in triplicate. *A* and *C*: ■, Cd39/Entpd1$^{-/-}$ mice; □, wild-type mice. *B* and *D*: □, without ATP; ■, with ATP. **$P < 0.05$; *$P > 0.05$ by ANOVA but $P < 0.05$ by Student's t test.

Interleukin-6, interleukin-1β, interferon-γ, and tumor necrosis factor-α levels are significantly higher in Cd39/Entpd1$^{-/-}$ mice than in wild-type mice (Table 1). NFκBp65 levels were also higher in the Cd39/Entpd1$^{-/-}$ mice liver treated with exogenous ATP (Cd39/Entpd1$^{-/-}$ mice 178.5 ± 24.1 vs. wild-type mice 100.0 ± 9.5 [arbitrary units]; $P = 0.0019$).

DISCUSSION

We have shown that deletion of Cd39/Entpd1 results in abnormalities of glucose homeostasis and causes insulin resistance. We show that the plasma insulin levels are higher in Cd39/Entpd1$^{-/-}$ mice than in wild-type mice during a GTT, and islets stain strongly for insulin in Cd39/Entpd1$^{-/-}$ mice tissues. Glucose intolerance in Cd39/Entpd1$^{-/-}$ mice does not appear to be related to an intrinsic abnormality in insulin secretion from β-cells. Significant effects of ATP administration on the GTT in contrast to other nucleotides suggest involvement of P2X receptors that are uniquely activated by ATP in the expression of glucose intolerance.

Cd39/Entpd1$^{-/-}$ mice are not obese, but leptin levels are increased. Leptin is an important anorexigenic hormone secreted from adipocytes (24–26). Insulin may induce secretion of leptin (27). Therefore, it is possible that the hyperinsulinemia of Cd39/Entpd1$^{-/-}$ mice might be a cause for hyperleptinemia. The food intake of Cd39/Entpd1$^{-/-}$ mice was comparable with those of wild-type mice despite the increased levels of plasma leptin. Leptin is also known to increase energy expenditure. However, calorimetric analysis of Cd39/Entpd1$^{-/-}$ mice revealed decreased heat generation and energy consumption both during dark and light cycles. Respiratory ratios of Cd39/Entpd1$^{-/-}$ mice were slightly lower than wild-type mice. Potentially, other tissue-specific mechanisms might exist for the regulation of energy consumption by extracellular

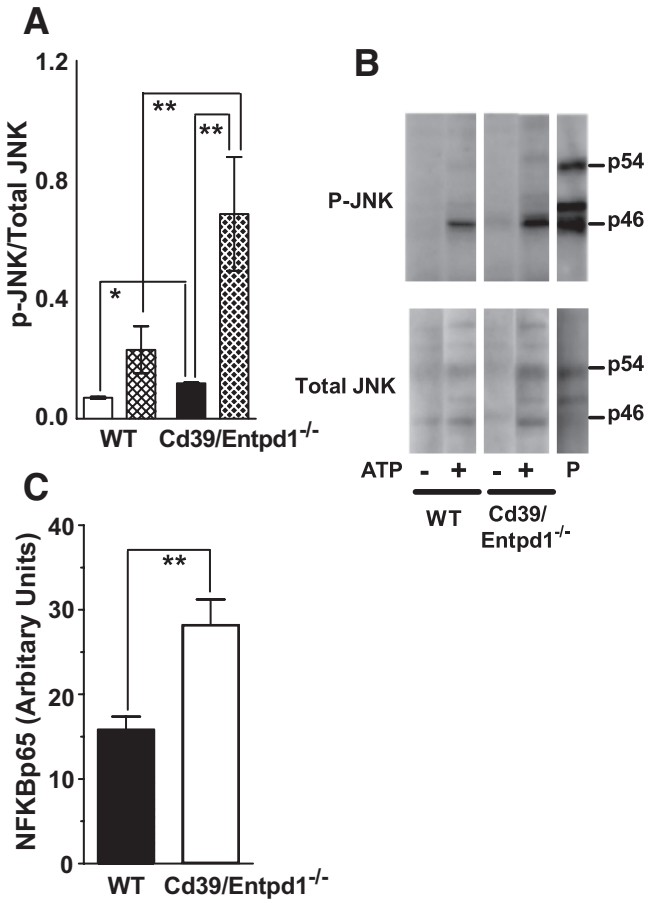

FIG. 6. c-JNK phosphorylation in murine liver. Mice were administered ATP via portal vein and the liver was harvested at 30 min after injection. The lysates were analyzed by Western blotting with anti–phospho-JNK antibodies or anti-JNK antibodies. *A*: Quantification of *p*-JNK to total JNK ratio by Western blot analysis. □, wild-type (WT) mice; ■, Cd39/Entpd1$^{-/-}$; ▨, ATP-treated mice (n = 3); solid bars, saline control mice. *B*: Representative staining of Western blot for *p*-JNK and JNK. P, a positive control. *C*: Quantification of NFKBp65 in murine liver nuclear extracts (n = 8–9). ■, wild-type (WT) mice; □, Cd39/Entpd1$^{-/-}$ mice. **$P < 0.05$; *$P > 0.05$ by ANOVA but $P < 0.05$ by Student's t test.

nucleotides. Our current data, however, suggest the possibility of both leptin resistance as well as insulin resistance in Cd39/Entpd1$^{-/-}$ mice.

Hyperinsulinemic-euglycemic clamp studies identified the liver as a major target organ for the effects of Cd39/Entpd1 on glucose homeostasis and insulin resistance. Immunohistochemical studies showing Cd39/Entpd1 to be expressed dominantly within the vasculature suggest that observed insulin resistance are secondary to modulation of extracellular and plasma nucleotides levels brought by loss of vascular ecto-nucleotidase activity. This is different mechanistically from the type of insulin resistance induced by a K121Q variant of PC-1 (ectonucleotide pyrophosphatase/phosphodiesterase). The latter requires direct/physical interactions between insulin receptor and PC-1 (28,29). Furthermore, PC-1 is expressed in skeletal muscle cells and hepatocytes unlike the unique vascular expression of Cd39/Entpd1.

We next examined aspects of glucose metabolism in primary hepatocyte cultures of Cd39/Entpd1$^{-/-}$ and wild-type mice. In general, glucose transport by hepatocytes is insulin-independent. However, expression of glucokinase is induced by insulin. We noted that the overall uptake of glucose was significantly decreased in Cd39/Entpd1$^{-/-}$ mice hepatocytes. Glucose uptake by wild-type primary culture hepatocyte was also significantly decreased by treatment with extracellular ATP, albeit not to the same extent as with Cd39/Entpd1$^{-/-}$ hepatocytes. ATP is known to induce hepatic gluconeogenesis (30) and impact upon glucose release via P2X4 receptor–mediated increases in glycogenolysis (31). Our and these published data suggest that the cellular phenotype seen in the Cd39/Entpd1$^{-/-}$ mice may be directly dependent upon exposure to extracellular nucleotides. We suggest that these are differential and persistent purinergic responses in these target tissues that are impacted upon by loss of Cd39/Entpd1 in vasculature. We infer that the reduced R_d values observed in Cd39/Entp1$^{-/-}$ mice during the hyperinsulinemic-euglycemic studies are secondary due, in substantial part, to the decreased glucose uptake in hepatocytes.

Other contributions of insulin to hepatic glucose homeostasis include the suppression of glucose production. Liver-specific insulin receptor knockout mice exhibit hepatic insulin resistance (i.e., impaired insulin-mediated suppression of hepatic glucose production that is accompanied by elevated plasma insulin levels). These features are also observed in Cd39/Entpd1$^{-/-}$ mice, suggesting indirect effects on insulin receptor activity (32).

Cd39/Entpd1$^{-/-}$ mice hepatocytes also show significantly higher basal glucose production than that seen in wild-type mice hepatocytes. Furthermore, the glucose production of Cd39/Entpd1$^{-/-}$ mice hepatocytes is not suppressed by the treatment of insulin, unlike in the instance of wild-type mice hepatocytes, in which this is suppressed by insulin. Interestingly, ATP treatment of wild-type hepatocytes also induces heightened hepatic glucose production, even in the presence of insulin. These results confirm that extracellular ATP regulates glucose homeostasis in hepatocytes. Furthermore, Cd39/Entpd1 expressed on adjacent cells, such as endothelial cells, is likely to regulate insulin signals in the hepatocyte by modulating extracellular nucleotide levels in the immediate microenvironment in vivo. It is worthy of mention that vascular endothelial-specific insulin receptor knockout mice do not exhibit insulin resistance (33). We propose that insulin resistance observed in Cd39/Entpd1$^{-/-}$ mice is not directly caused by modulation of vasculature functions but involves other factors (e.g., paracrine fluxes of extracellular nucleotides that impact target tissues such as the hepatocyte).

Activation of cellular signaling cascades by proinflammatory cytokines such as tumor necrosis factor-α and interleukin-1, free fatty acids, or nucleotides (14) can also induce cellular activation via inflammatory kinases. Activation of inflammatory kinases, such as c-JNK, also cause aberrant serine phosphorylation of IRS. This specific form of serine phosphorylation prevents consequent tyrosine phosphorylation by insulin receptors and association of phosphoinositide 3-kinases, leading to impaired insulin signal transduction (34,35).

To analyze the molecular mechanisms for insulin resistance of Cd39/Entpd1$^{-/-}$ mice, we analyzed tyrosine phosphorylation of IRS-1 and -2. Insulin-stimulated tyrosine phosphorylation of IRS-2 was significantly decreased in Cd39/Entpd1$^{-/-}$ mice liver. In addition, phosphorylation of c-JNK induced by administration of ATP was also significantly increased in Cd39/Entpd1$^{-/-}$ mice liver. These data suggest that insulin resistance of Cd39/Entpd1$^{-/-}$ mice is associated with increased activation of hepatic c-JNK/SAP by extracellular ATP. This likely results

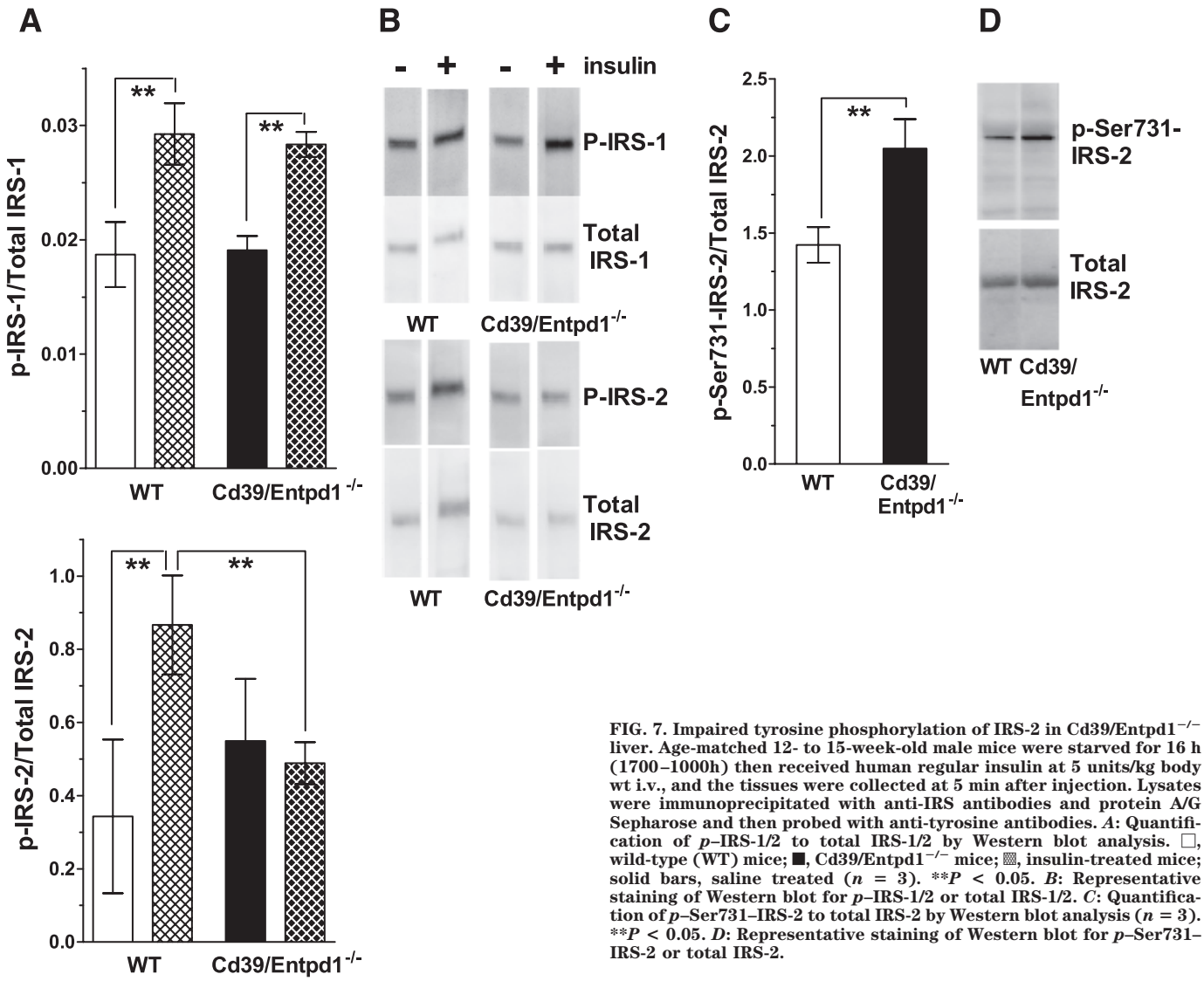

FIG. 7. Impaired tyrosine phosphorylation of IRS-2 in Cd39/Entpd1$^{-/-}$ liver. Age-matched 12- to 15-week-old male mice were starved for 16 h (1700–1000h) then received human regular insulin at 5 units/kg body wt i.v., and the tissues were collected at 5 min after injection. Lysates were immunoprecipitated with anti-IRS antibodies and protein A/G Sepharose and then probed with anti-tyrosine antibodies. *A*: Quantification of *p*–IRS-1/2 to total IRS-1/2 by Western blot analysis. □, wild-type (WT) mice; ■, Cd39/Entpd1$^{-/-}$ mice; ▨, insulin-treated mice; solid bars, saline treated (n = 3). **P < 0.05. *B*: Representative staining of Western blot for *p*–IRS-1/2 or total IRS-1/2. *C*: Quantification of *p*–Ser731–IRS-2 to total IRS-2 by Western blot analysis (n = 3). **P < 0.05. *D*: Representative staining of Western blot for *p*–Ser731–IRS-2 or total IRS-2.

in aberrant serine phosphorylation and consequently decreased tyrosine phosphorylation of IRS-2. Similar patterns of aberrant IRS-2 phosphorylation have been noted in other insulin resistance states (36).

Furthermore, several features observed in Cd39/Entpd1$^{-/-}$ mice are also seen in IRS-2$^{-/-}$ mice: both show elevated plasma insulin levels and have normal fasting blood glucose levels with impaired glucose homeostasis in the liver. IRS-2$^{-/-}$ mice, however, show increases in blood glucose levels with advancing age due to lack of compensatory β-cell hyperplasia (37).

Other cellular candidates for mediating insulin resistance of Cd39/Entpd1$^{-/-}$ mice include immune cells such as macrophages in adipose tissues and the Kupffer cells of the liver, as alluded to above (35). Activation of purinergic signaling pathways is already known to induce secretion of cytokines from both immune and endothelial cells (38–42). We show that serum proinflammatory cytokine levels (interleukin-1β, interleukin-6, interferon-γ, and tumor necrosis factor-α) are significantly higher in Cd39/Entpd1$^{-/-}$ mice than in wild-type mice. Accordingly, hypersecretion of select cytokines by monocytes and other cells also might contribute, at least in part, to the development of insulin resistance in Cd39/Entpd1$^{-/-}$ mice.

Our data suggest that insulin resistance in Cd39/NTPDase1$^{-/-}$ mice is associated with disordered extracellular nucleotide signaling that directly impacts important metabolic pathways in hepatocytes via aberrant IRS-2 phosphorylation. However, we do not exclude the possibility that deletion of Cd39 might also contribute to insulin resistance in a somewhat more indirect manner via the induction of inflammatory cytokines. The relative contributions of these two nonexclusive mechanisms remain to be determined.

We have already reported on other vascular and immune abnormalities in Cd39/Entpd1$^{-/-}$ mice. This described phenotype includes disordered thromboregulation, aberrant inflammatory responses, impaired angiogenesis and regeneration of the liver, impaired function of regulatory T-cells, and predisposition to diabetic renal diseases with increased proteinuria and hypertension (3,5,12,15,42). To these manifestations of Cd39/Entpd1 deletion, we now add metabolic consequences.

In conclusion, Cd39/Entpd1 expressed by the vasculature and by immune cells serves as an important modulator of hepatic carbohydrate metabolism. The pathogenetic mechanism involves failure to control extracellular nucle-

otide fluxes that both directly and indirectly impact insulin responsiveness.

ACKNOWLEDGMENTS

This work was supported by American Heart Association Grant AHA 0530362N (to K.E.); by National Institutes of Health Grants NIH HL063972 (to S.C.R.), HL076540 (to S.C.R.), and NIDDK 43051 (to B.B.K); and an American Diabetes Association Mentor-Based Fellowship (to B.B.K.).

REFERENCES

1. Bours MJ, Swennen EL, Di Virgilio F, Cronstein BN, Dagnelie PC: Adenosine 5′-triphosphate and adenosine as endogenous signaling molecules in immunity and inflammation. *Pharmacol Ther* 112:358–404, 2006
2. Volonte C, Amadio S, D'Ambrosi N, Colpi M, Burnstock G: P2 receptor web: complexity and fine-tuning. *Pharmacol Ther* 112:264–280, 2006
3. Enjyoji K, Sevigny J, Lin Y, Frenette PS, Christie PD, Esch JS, 2nd, Imai M, Edelberg JM, Rayburn H, Lech M, Beeler DL, Csizmadia E, Wagner DD, Robson SC, Rosenberg RD: Targeted disruption of cd39/ATP diphosphohydrolase results in disordered hemostasis and thromboregulation. *Nat Med* 5:1010–1017, 1999
4. Goepfert C, Sundberg C, Sevigny J, Enjyoji K, Hoshi T, Csizmadia E, Robson S: Disordered cellular migration and angiogenesis in cd39-null mice. *Circulation* 104:3109–3115, 2001
5. Mizumoto N, Kumamoto T, Robson SC, Sevigny J, Matsue H, Enjyoji K, Takashima A: CD39 is the dominant Langerhans cell-associated ecto-NTPDase: modulatory roles in inflammation and immune responsiveness. *Nat Med* 8:358–365, 2002
6. Chevassus H, Roig A, Belloc C, Lajoix AD, Broca C, Manteghetti M, Petit P: P2Y receptor activation enhances insulin release from pancreatic beta-cells by triggering the cyclic AMP/protein kinase A pathway. *Naunyn Schmiedebergs Arch Pharmacol* 366:464–469, 2002
7. Fernandez-Alvarez J, Hillaire-Buys D, Loubatieres-Mariani MM, Gomis R, Petit P: P2 receptor agonists stimulate insulin release from human pancreatic islets. *Pancreas* 22:69–71, 2001
8. Poulsen CR, Bokvist K, Olsen HL, Hoy M, Capito K, Gilon P, Gromada J: Multiple sites of purinergic control of insulin secretion in mouse pancreatic β-cells. *Diabetes* 48:2171–2181, 1999
9. Kim MS, Lee J, Ha J, Kim SS, Kong Y, Cho YH, Baik HH, Kang I: ATP stimulates glucose transport through activation of P2 purinergic receptors in C(2)C(12) skeletal muscle cells. *Arch Biochem Biophys* 401:205–214, 2002
10. Solini A, Chiozzi P, Morelli A, Passaro A, Fellin R, Di Virgilio F: Defective P2Y purinergic receptor function: a possible novel mechanism for impaired glucose transport. *J Cell Physiol* 197:435–444, 2003
11. Ferrari D, Pizzirani C, Adinolfi E, Lemoli RM, Curti A, Idzko M, Panther E, Di Virgilio F: The P2X7 receptor: a key player in IL-1 processing and release. *J Immunol* 176:3877–3883, 2006
12. Deaglio S, Dwyer KM, Gao W, Friedman D, Usheva A, Erat A, Chen JF, Enjyoji K, Linden J, Oukka M, Kuchroo VK, Strom TB, Robson SC: Adenosine generation catalyzed by CD39 and CD73 expressed on regulatory T cells mediates immune suppression. *J Exp Med* 204:1257–1265, 2007
13. Robinson WP 3rd, Douillet CD, Milano PM, Boucher RC, Patterson C, Rich PB: ATP stimulates MMP-2 release from human aortic smooth muscle cells via JNK signaling pathway. *Am J Physiol Heart Circ Physiol* 290:H1988–H1996, 2006
14. Thevananther S, Sun H, Li D, Arjunan V, Awad SS, Wyllie S, Zimmerman TL, Goss JA, Karpen SJ: Extracellular ATP activates c-jun N-terminal kinase signaling and cell cycle progression in hepatocytes. *Hepatology* 39:393–402, 2004
15. Friedman DJ, Rennke HG, Csizmadia E, Enjyoji K, Robson SC: The vascular ectonucleotidase ENTPD1 is a novel renoprotective factor in diabetic nephropathy. *Diabetes* 56:2371–2379, 2007
16. Aguirre V, Uchida T, Yenush L, Davis R, White MF: The c-Jun NH(2)-terminal kinase promotes insulin resistance during association with insulin receptor substrate-1 and phosphorylation of Ser(307). *J Biol Chem* 275: 9047–9054, 2000
17. Ishizuka T, Kajita K, Natsume Y, Kawai Y, Kanoh Y, Miura A, Ishizawa M, Uno Y, Morita H, Yasuda K: Protein kinase C (PKC) beta modulates serine phosphorylation of insulin receptor substrate-1 (IRS-1): effect of overexpression of PKCbeta on insulin signal transduction. *Endocr Res* 30:287–299, 2004
18. Kotani K, Peroni OD, Minokoshi Y, Boss O, Kahn BB: GLUT4 glucose transporter deficiency increases hepatic lipid production and peripheral lipid utilization. *J Clin Invest* 114:1666–1675, 2004
19. Nagy TR, Clair AL: Precision and accuracy of dual-energy X-ray absorptiometry for determining in vivo body composition of mice. *Obes Res* 8:392–398, 2000
20. Harman AW, McCamish LE, Henry CA: Isolation of hepatocytes from postnatal mice. *J Pharmacol Methods* 17:157–163, 1987
21. Pedersen TA, Bereshchenko O, Garcia-Silva S, Ermakova O, Kurz E, Mandrup S, Porse BT, Nerlov C: Distinct C/EBPalpha motifs regulate lipogenic and gluconeogenic gene expression in vivo. *EMBO J* 26:1081–1093, 2007
22. Beldi G, Wu Y, Banz Y, Nowak M, Miller L, Enjyoji K, Yegutkin GG, Candinas D, Exley M, Robson SC: NKT cell dysfunction in CD39/Entpd1 null mice protects against concanavalin A-induced hepatitis. *Hepatology*, 2008. In press
23. Dranoff JA, Kruglov EA, Robson SC, Braun N, Zimmermann H, Sevigny J: The ecto-nucleoside triphosphate diphosphohydrolase NTPDase2/CD39L1 is expressed in a novel functional compartment within the liver. *Hepatology* 36:1135–1144, 2002
24. Lee JH, Reed DR, Price RA: Leptin resistance is associated with extreme obesity and aggregates in families. *Int J Obes Relat Metab Disord* 25:1471–1473, 2001
25. Rahmouni K, Morgan DA, Morgan GM, Mark AL, Haynes WG: Role of selective leptin resistance in diet-induced obesity hypertension. *Diabetes* 54:2012–2018, 2005
26. Shimizu H, Oh IS, Okada S, Mori M: Leptin resistance and obesity. *Endocr J* 54:17–26, 2007
27. Cammisotto PG, Gelinas Y, Deshaies Y, Bukowiecki LJ: Regulation of leptin secretion from white adipocytes by insulin, glycolytic substrates, and amino acids. *Am J Physiol Endocrinol Metab* 289:E166–E171, 2005
28. Stefan C, Wera S, Stalmans W, Bollen M: The inhibition of the insulin receptor by the receptor protein PC-1 is not specific and results from the hydrolysis of ATP. *Diabetes* 45:980–983, 1996
29. Maddox BA, Goldfine ID: Membrane glycoprotein PC-1 inhibition of insulin receptor function occurs via direct interaction with the receptor α-subunit. *Diabetes* 49:13–19, 2000
30. Koike M, Kashiwagura T, Takeguchi N: Gluconeogenesis stimulated by extracellular ATP is triggered by the initial increase in the intracellular Ca2+ concentration of the periphery of hepatocytes. *Biochem J* 283:265–272, 1992
31. Emmett DS, Feranchak A, Kilic G, Puljak L, Miller B, Dolovcak S, McWilliams R, Doctor RB, Fitz JG: Characterization of ionotrophic purinergic receptors in hepatocytes. *Hepatology* 47:698–705, 2008
32. Michael MD, Kulkarni RN, Postic C, Previs SF, Shulman GI, Magnuson MA, Kahn CR: Loss of insulin signaling in hepatocytes leads to severe insulin resistance and progressive hepatic dysfunction. *Mol Cell* 6:87–97, 2000
33. Vicent D, Ilany J, Kondo T, Naruse K, Fisher SJ, Kisanuki YY, Bursell S, Yanagisawa M, King GL, Kahn CR: The role of endothelial insulin signaling in the regulation of vascular tone and insulin resistance. *J Clin Invest* 111:1373–1380, 2003
34. Hotamisligil GS: Inflammation and metabolic disorders. *Nature* 444:860–867, 2006
35. Shoelson SE, Lee J, Goldfine AB: Inflammation and insulin resistance. *J Clin Invest* 116:1793–1801, 2006
36. Scioscia M, Gumaa K, Kunjara S, Paine MA, Selvaggi LE, Rodeck CH, Rademacher TW: Insulin resistance in human preeclamptic placenta is mediated by serine phosphorylation of insulin receptor substrate-1 and -2. *J Clin Endocrinol Metab* 91:709–717, 2006
37. Kubota N, Tobe K, Terauchi Y, Eto K, Yamauchi T, Suzuki R, Tsubamoto Y, Komeda K, Nakano R, Miki H, Satoh S, Sekihara H, Sciacchitano S, Lesniak M, Aizawa S, Nagai R, Kimura S, Akanuma Y, Taylor SI, Kadowaki T: Disruption of insulin receptor substrate 2 causes type 2 diabetes because of liver insulin resistance and lack of compensatory β-cell hyperplasia. *Diabetes* 49:1880–1889, 2000
38. Lumeng CN, Bodzin JL, Saltiel AR: Obesity induces a phenotypic switch in adipose tissue macrophage polarization. *J Clin Invest* 117:175–184, 2007
39. Inoue K, Hosoi J, Denda M: Extracellular ATP has stimulatory effects on the expression and release of IL-6 via purinergic receptors in normal human epidermal keratinocytes. *J Invest Dermatol* 127:362–371, 2007
40. Hide I, Tanaka M, Inoue A, Nakajima K, Kohsaka S, Inoue K, Nakata Y: Extracellular ATP triggers tumor necrosis factor-alpha release from rat microglia. *J Neurochem* 75:965–972, 2000
41. Hanley PJ, Musset B, Renigunta V, Limberg SH, Dalpke AH, Sus R, Heeg KM, Preisig-Muller R, Daut J: Extracellular ATP induces oscillations of intracellular Ca2+ and membrane potential and promotes transcription of IL-6 in macrophages. *Proc Natl Acad Sci U S A* 101:9479–9484, 2004
42. Dwyer KM, Deaglio S, Gao W, Friedman D, Strom TB, Robson SC: CD39 and control of cellular immune responses. *Purinergic Signal* 3:171–180, 2007